MAJOR ARTICLE

Indian Ocean Dipole and Rainfall Drive a Moran Effect in East Africa Malaria Transmission

Luis Fernando Chaves,[1,2] Akiko Satake,[1] Masahiro Hashizume,[3] and Noboru Minakawa[3]

[1]Graduate School of Environmental Sciences and Global Center of Excellence Program on Integrated Field Environmental Science, Hokkaido University, Sapporo; [2]Programa de Investigación en Enfermedades Tropicales, Escuela de Medicina Veterinaria, Universidad Nacional, Heredia, Costa Rica; and [3]Institute of Tropical Medicine (NEKKEN) and Global Center of Excellence Program on Tropical and Emergent Infectious Diseases, Nagasaki University, Japan

Background. Patterns of concerted fluctuation in populations—synchrony—can reveal impacts of climatic variability on disease dynamics. We examined whether malaria transmission has been synchronous in an area with a common rainfall regime and sensitive to the Indian Ocean Dipole (IOD), a global climatic phenomenon affecting weather patterns in East Africa.

Methods. We studied malaria synchrony in 5 15-year long (1984–1999) monthly time series that encompass an altitudinal gradient, approximately 1000 m to 2000 m, along Lake Victoria basin. We quantified the association patterns between rainfall and malaria time series at different altitudes and across the altitudinal gradient encompassed by the study locations.

Results. We found a positive seasonal association of rainfall with malaria, which decreased with altitude. By contrast, IOD and interannual rainfall impacts on interannual disease cycles increased with altitude. Our analysis revealed a nondecaying synchrony of similar magnitude in both malaria and rainfall, as expected under a Moran effect, supporting a role for climatic variability on malaria epidemic frequency, which might reflect rainfall-mediated changes in mosquito abundance.

Conclusions. Synchronous malaria epidemics call for the integration of knowledge on the forcing of malaria transmission by environmental variability to develop robust malaria control and elimination programs.

Synchrony, the degree of concerted fluctuations among populations in a region, is a key parameter to understand impacts of climatic trends and variability on population dynamics [1]. For infectious diseases, synchrony has become especially important because its estimation offers a mean to test hypotheses regarding the importance of exogenous epidemic drivers. In a relatively homogenous environment, a synchrony decay with distance implies that impacts of climatic trends and variability, if any, are marginal when compared with regulatory factors related to population processes (eg, immunity in diseases) and independent of the changing environment [2]. By contrast, a nondecaying synchrony of magnitude slightly larger than or similar to that of the environment will support a Moran effect, in which transmission patterns in a region could be similar by a common mechanism of action for the exogenous, often climatic, forcing [3]. As originally defined, the Moran effect arises by the emerging synchronization of autoregressive dynamics of time series by the impact of common sources of exogenous forcing (ie, the autonomous [or endogenous] dynamics of a population get tuned to that of external factors influencing the dynamics of populations living under a similar [or correlated] environment) [2].

Vector-borne diseases, such as malaria, are excellent model systems to study synchrony and test Moran effects. For example, Moran effects are expected in malaria because of the monotonic relationship

Received 19 July 2011; accepted 29 December 2011; electronically published 5 April 2012.

Correspondence: Luis Fernando Chaves, Lic, MSc, PhD, Graduate School of Environmental Sciences, Hokkaido University, Rm A701 5-chome, Kita 10-jo Nishi, Kita-ku, Sapporo 060-0810, Hokkaido, Japan (lchaves@ees.hokudai.ac.jp).

The Journal of Infectious Diseases 2012;205:1885–91

DOI: 10.1093/infdis/jis289

between vector abundance and transmission [4] and between vectors and rainfall [5]. Lake Victoria basin (LVB) is a unique setting to study exogenous forcing in malaria transmission because of three main reasons:

1. It encompasses an altitudinal gradient, which is also a gradient of malaria endemicity [6, 7].
2. It has relatively homogeneous rainfall patterns [8].
3. Rainfall and malaria are impacted by global climatic phenomena, especially the Indian Ocean Dipole (IOD), an irregular oscillation of sea-surface temperatures in which the western Indian Ocean becomes alternately warmer and then colder than the eastern part of the ocean [9, 10].

Here, we studied malaria synchrony in 5 15-year long (1984–1999) monthly time series (Figure 1*A*) from LVB, west Kenya (Figure 2). We also studied rainfall time series (Figure 1*B*) synchrony to test the condition of environmental autocorrelation necessary for a Moran effect. We used the dipole mode index (DMI) (Figure 1*C*) as an IOD index [11] to

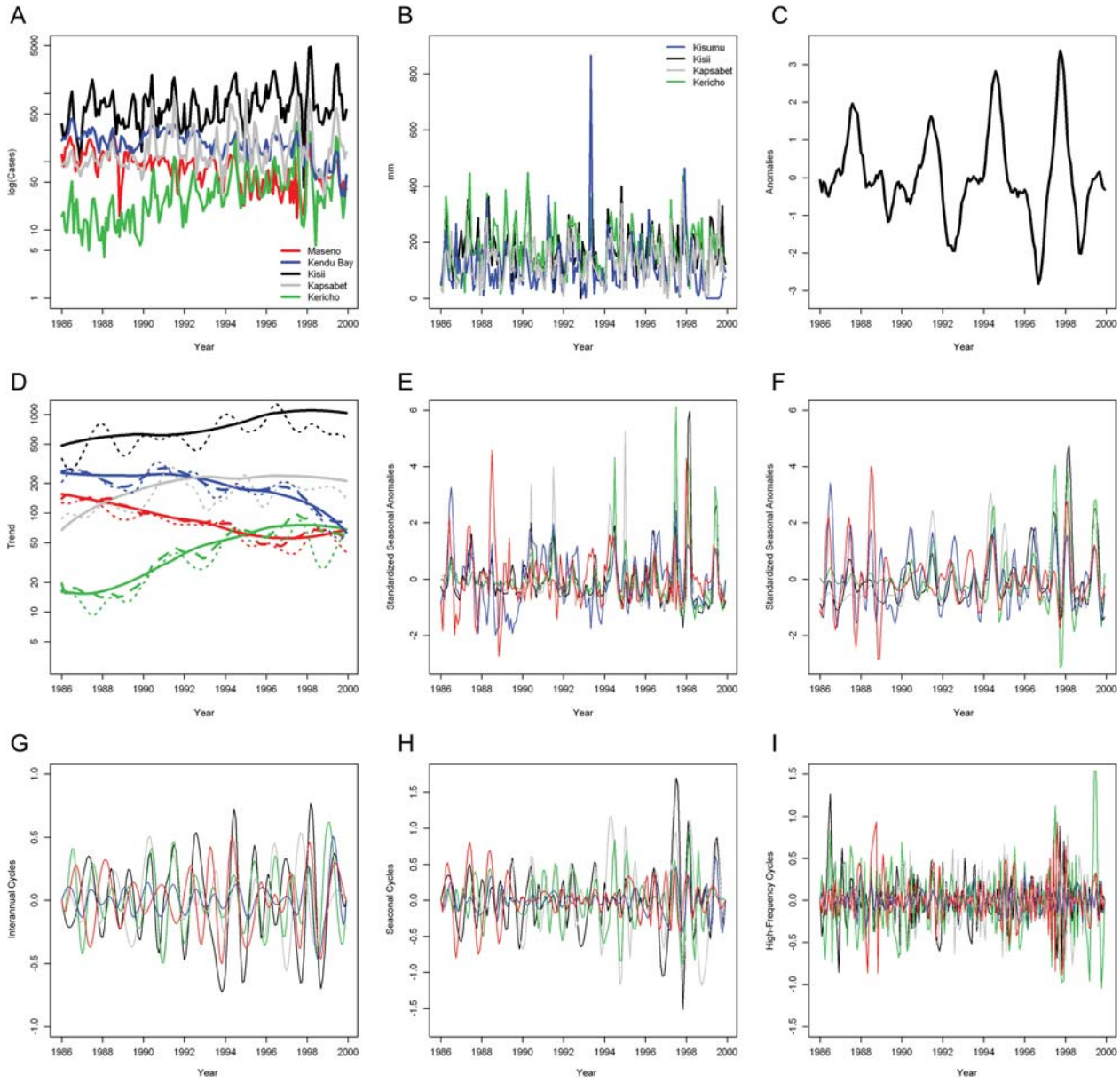

Figure 1. Data for malaria time series (*A*), rainfall (*B*), dipole mode index (*C*), and trends (*D*). Solid lines are for Loess, dashed lines are for singular spectrum analysis (SSA), and dotted lines are for empirical mode decomposition. There is no dashed line for Kisii and Kapsabet because the SSA was unable to detect any trends. *E*, Loess detrended malaria time series. *F*, SSA detrended malaria time series. *G*, Malaria intrinsic mode functions (IMFs) with interannual cycles. *H*, Malaria IMFs with seasonal cycles. *I*, Malaria IMFs with high-frequency cycles. Color codes are shared by panels *A*, *D*, *E*, *F*, *G*, *H*, and *I*. The IMFs were derived via an EMD for each time series.

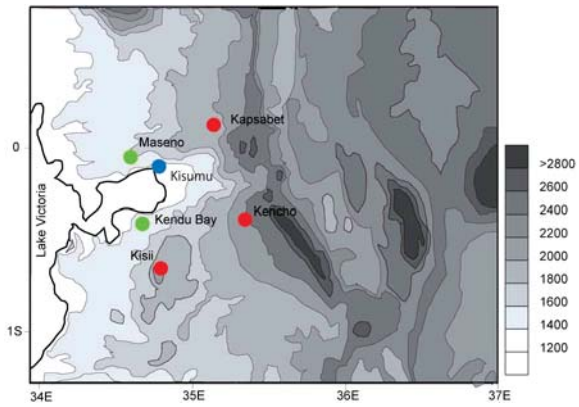

Figure 2. Study sites in Lake Victoria basin, western Kenya. Kisumu (0°6′S 34°45′E; altitude = 1131 m); Kendu Bay (0°24′05″S, 34°39′56″E; altitude = 1240 m); Maseno (0°00′15″S, 34°36′16″E; altitude = 1500 m); Kisii (0°40′S, 34°46′E; altitude = 1670 m); Kapsabet (0°12′N, 35°06′E; altitude = 2000 m); Kericho (0°23′55″N, 35°15′30″E; altitude = 2000 m). On the map, elevation is measured in meters and indicated by gray color. Location color indicates the data available at each site: blue = rainfall; green = disease; and red = disease and rainfall.

quantify its role as interannual driver of malaria and rainfall dynamics. We found that both rainfall and malaria had a non-decaying synchrony with distance and that malaria synchrony was slightly larger than rainfall synchrony, as expected under a Moran effect. A more detailed time scale analysis of synchrony showed that seasonal cycles in malaria transmission were led by 2-month lagged changes in rainfall, with decreasing intensity as a function of altitude. By contrast, interannual cycles in the disease were driven by IOD, with an increasing intensity with altitude. These patterns could be related to the population dynamics of *Anopheles* mosquitoes, whose abundance is likely driven by rainfall patterns in the region [5, 12]. Finally, our results clearly show that patterns of climatic variability have a strong signature in malaria transmission among vulnerable populations and are, therefore, a necessary input for a strong malaria control/elimination framework.

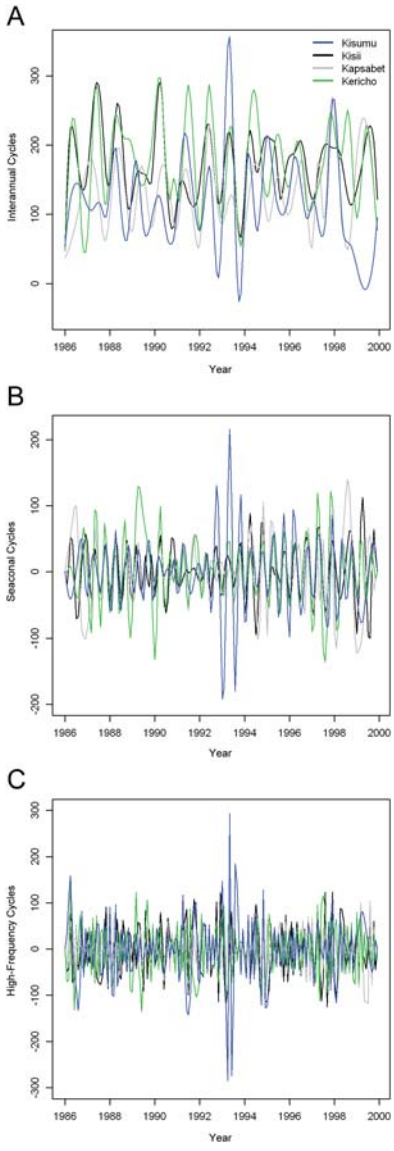

Figure 3. Rainfall empirical model decomposition time series. *A,* Intrinsic mode functions (IMFs) with interannual cycles. *B,* IMFs with seasonal cycles. *C,* IMFs with high-frequency cycles.

MATERIALS AND METHODS

Data

Malaria and rainfall data spanned from January 1985 to December 1999. The 5 malaria time series were monthly counts of inpatients admitted into the hospitals because of high fever and other clinical malaria symptoms. In Kericho, all malaria cases were confirmed by blood slide examination [13]. At the other 4 sites (Maseno, Kendu Bay, Kisii, and Kapsabet), we collected the data from books with malaria-diagnosed inpatient records. Unfortunately, these books did not indicate whether all recorded malaria cases were confirmed by blood slide examination. However, we were informed by staff members from each hospital that cases were often confirmed by blood slide examination. We restricted our samples to this kind of malaria infection (ie, inpatient admissions) in order to make a sound statistical analysis at the price of using data that likely underestimate the total number of malaria infections [14]. Rainfall data were obtained from the Kenyan Meteorological Service. We used rainfall records from some of the same locations of the malaria time series and a location midway between the 2 lowest altitude sites (Figure 2). Specifically, we employed meteorological records from Kisumu as proxy inputs for Kendu Bay and Maseno, localities for which we were unable to find relatively complete records through the Kenyan Meteorological Service and other meteorological data repositories. We chose Kisumu

Table 1. Confidence Intervals for the Regional Synchrony Estimates

Time Series	Mean ± SE	95% Confidence Intervals
Malaria, Loess	0.48 ± 0.06	.34–.61
Malaria, SSA	0.53 ± 0.05	.42–.64
Malaria, EMD	0.49 ± 0.03	.42–.56
Rainfall, raw data	0.52 ± 0.06	.37–.66
Rainfall, EMD	0.43 ± 0.03	.34–.51

The 95% confidence intervals were estimated from the standard error (SE) of maximum likelihood estimates for the regional synchrony.

Abbreviations: EMD, empirical mode decomposition; SSA, singular spectrum analysis.

because of the lack of missing observations during the study period and because of the similar rainfall patterns to Kendu Bay and Maseno according to meteorological models [8].

Statistical Analysis

To estimate synchrony in the time series, we first removed nonstationary trends [15] in the malaria time series (Figure 1*D*) using 3 standard procedures: local polynomial regression fitting (Loess) [15], singular spectrum analysis (SSA) [16], and empirical mode decomposition (EMD) [17]. These methods have different assumptions and outcomes, Loess extracts (non)linear trends (Figure 1*E*), whereas SSA (Figure 1*F*) and EMD decompose signals into different oscillatory (Figure 1*G–I*) and noncyclical components. In SSA, the trends are extracted by examining the variability of the largest eigenvalue from an autocovariance matrix, whereas EMD decomposes a time series by building oscillatory signals—intrinsic mode functions (IMF)—that are repeatedly subtracted from the time series. We employed these different methods to ensure robustness in the inferences from subsequent analyses. The lack of nonstationary trends in rainfall made unnecessary

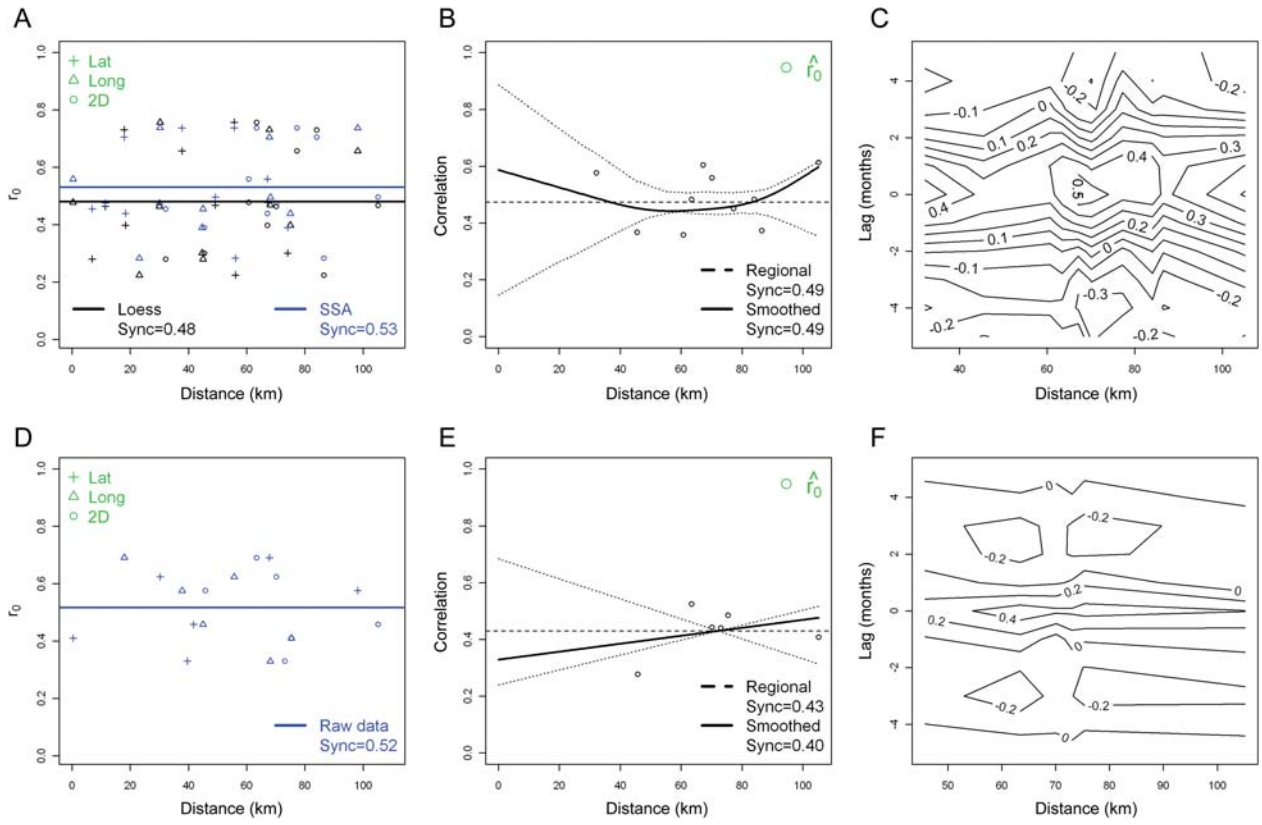

Figure 4. Synchrony analysis. *A,* Malaria time series correlation at lag 0 (r_0) as function of latitude (Lat), longitude (Long), and 2-dimensional distance (2D) between the studied localities. Colors indicate the method employed to detrend the malaria time series employed to estimate r_0. *B,* Two-dimensional distance spline correlogram (3 edf) for the signal obtained by adding the seasonal and interannual intrinsic mode functions from the empirical mode decomposition (EMD) applied to the malaria time series. *C,* Contour map for temporal cross-correlations between the EMD detrended malaria time series. *D,* Rainfall time series correlation at lag 0 (r_0) as function of Lat, Long, and 2D distance between the studied localities. *E,* Two-dimensional distance spline correlogram (2 edf) for the signal obtained by adding the seasonal and interannual intrinsic mode functions from the empirical mode decomposition applied to the rainfall time series. *F,* Contour map for temporal cross-correlations among the rainfall time series. In *A, B, D,* and *E,* Synch is the estimated regional synchrony obtained with each method. In *B* and *E,* dotted lines indicate the 95% confidence intervals for the smoothed correlation function (solid line) obtained with 1000 data permutations. In *C* and *F,* the y-axis represents the lag for the cross correlation and the x-axis represents the 2D distance. Values in the contour lines are correlations, which are significantly different from 0 when their absolute value is >0.075 ($P < .05$).

the treatment with Loess and SSA. However, we decomposed rainfall data using EMD to perform frequency-specific association analysis (Figure 3). Second, we estimated the synchrony (r_0) (ie, cross correlation at lag 0) of rainfall and detrended malaria time series using both linear regression [2] and spline correlogram on high-frequency filtered, detrended time series [18]. Third, we studied the association between rainfall and DMI with malaria along the altitudinal gradient of our study locations using cross-correlation functions [15]. Further details about the data and methods are presented in the Supplementary Data.

RESULTS

Estimates for malaria regional synchrony (Table 1) were similar using SSA, Loess (Figure 4*A*), and EMD (Figure 4*B*) detrended time series. Malaria time series synchronicity was observed across the 2-dimensional distance and altitude (gradients) with all series in phase and with their maximum correlation observed at lag 0 (Figure 4*C*), with minimum correlations well above 0.3 at lag 0 in the EMD detrended malaria data (Figure 4*B* and 4*C*; Table 1). For rainfall, synchrony estimates from the raw time series (Figure 4*D*) and EMD (Figure 4*E*) were very similar across the range of distances and altitudes studied (Figure 4*F*). To estimate the smoothed correlogram of malaria (Figure 4*B*) and rainfall (Figure 4*E*), we employed only the EMD detrended time series because this procedure also allowed us to filter out high-frequency components in the time series, which can artificially increase time series synchrony by the emerging correlation expected from high-frequency band constraints. The smoothed correlograms for both malaria (Figure 4*B*) and rainfall (Figure 4*E*) were similar to the regional synchrony, as the 95% confidence interval contained the smoothed correlogram along the range of studied distances in each case (Figure 4*B* and 4*E*). Similarly, as expected under a Moran effect, the regional malaria and rainfall synchrony patterns were not statistically different (Table 1). Two-month lagged rainfall had the highest positive

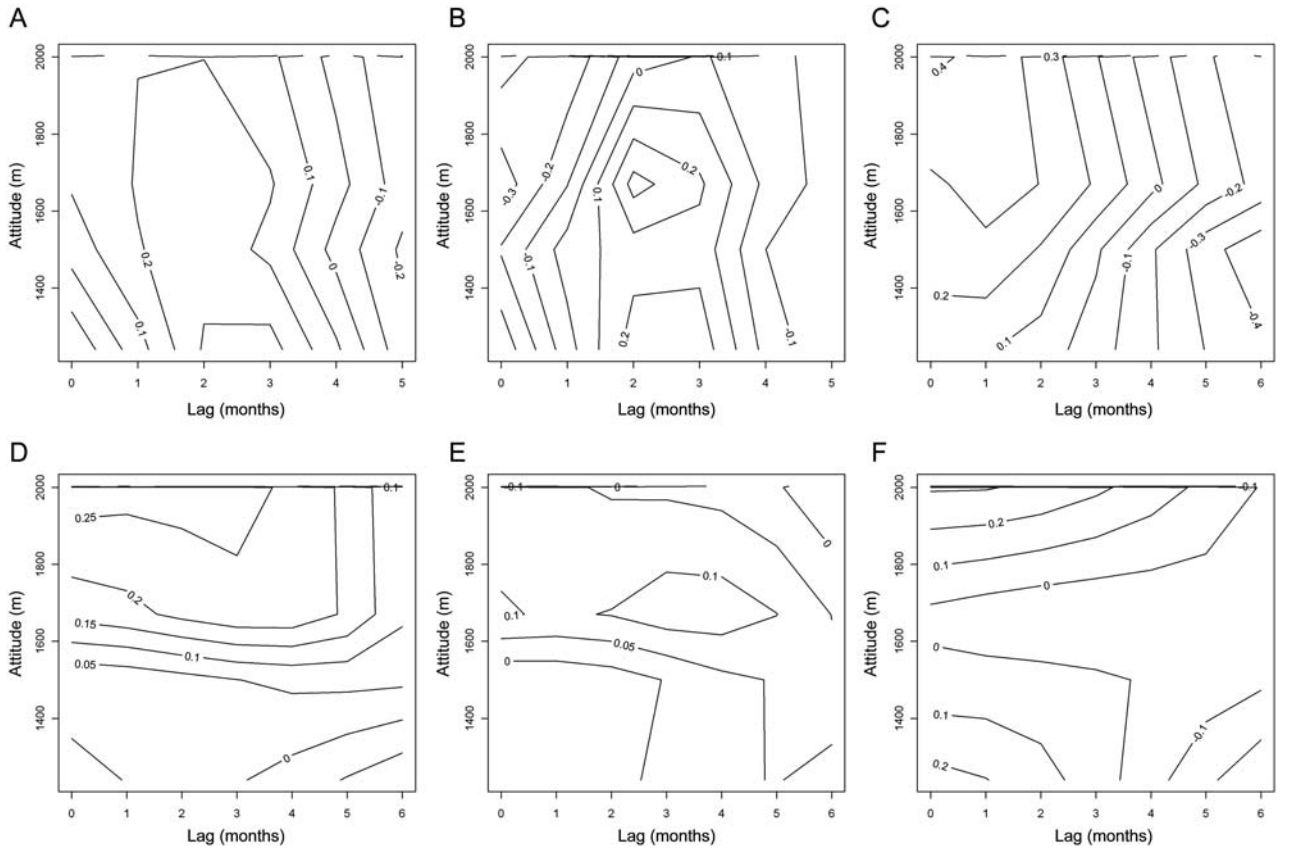

Figure 5. Time scale impacts of rainfall and Indian Ocean Dipole on malaria synchrony across an altitude gradient. *A,* Singular spectrum analysis (SSA) detrended malaria time series correlation with rainfall. *B,* Seasonal malaria intrinsic mode function (IMF) correlation with seasonal rainfall IMF. *C,* Interannual malaria IMF correlation with interannual rainfall IMF. *D,* SSA detrended malaria correlation with dipole mode index (DMI). *E,* Seasonal malaria IMF correlation with DMI. *F,* Interannual malaria IMF correlation with DMI. The IMFs for each malaria time series were obtained by empirical mode decompositions. In all panels, the x-axis represents the lag for the cross correlation and the y-axis represents the site altitude. Values in the contour lines are correlations, which are significantly different from 0 when their absolute value is >0.075 ($P < .05$).

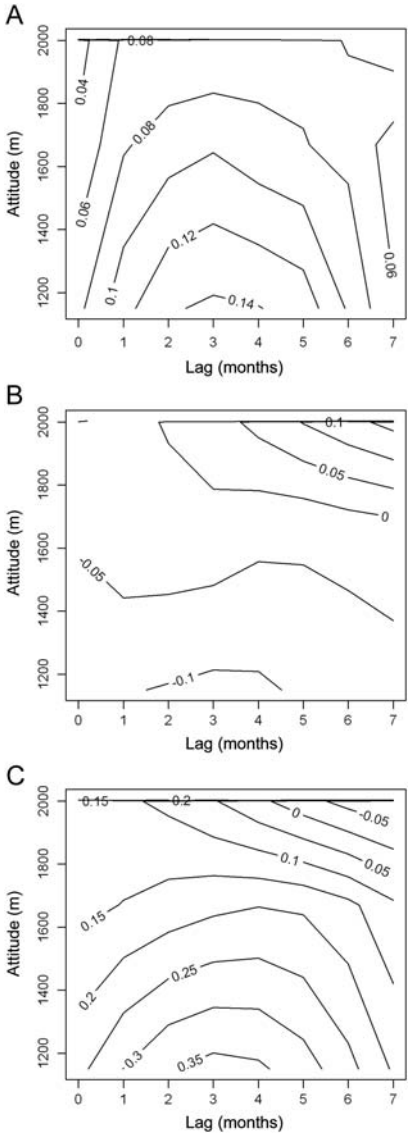

Figure 6. Time scale association between rainfall and dipole mode Index (DMI). *A*, Rainfall correlation with DMI. *B*, Seasonal rainfall intrinsic mode function (IMF) correlation with DMI. *C*, Interannual rainfall IMF correlation with DMI. The IMFs for each malaria time series were obtained by empirical mode decompositions. The x-axis represents the lag for the cross correlation and the y-axis represents the site altitude. Values in the contour lines are correlations, which are significantly different from 0 when their absolute value is >0.075 ($P < .05$).

correlation with malaria, with a decreasing association as function of increasing elevation (Figure 5*A*), a pattern also observed for an analysis based only on the EMD-extracted seasonal malaria IMFs (Figure 5*B*). The consideration of EMD extracted interannual malaria IMFs (Figure 5*C*) showed the association between interannual rainfall and interannual malaria to have a maximum positive correlation when rainfall is 1-month lagged in relation with malaria, and a maximum negative correlation when rainfall is 4-month lagged in relation with malaria, suggesting a role for rainfall temporal variability in the synchronous malaria dynamics. The SSA detrended malaria-DMI cross correlation function (Figure 5*D*) showed the positive association between these time series was maximum for up to 4 months of lagged DMI at altitudes >1600 m. When the seasonal (Figure 5*E*) and interannual (Figure 5*F*) malaria IMF were correlated with DMI, the association up to 4 months of lagged DMI showed to be robust at interannual scales and altitudes >1600 m. In addition, the analysis with the IMFs also showed that DMI and seasonal components of malaria are associated at seasonal scales for 3 and 4 months of lagged DMI (Figure 5*E*) and the association between DMI and malaria can be continuous along the altitudinal gradient given the emergence of significant patterns of association at altitudes <1600 m and >1600 m (Figure 5*F*). Patterns of association between malaria and DMI could be mediated by the impact of DMI on rainfall. Dipole mode index and rainfall have a correlation that decreases with altitude, which is maximized between 2 and 6 months (Figure 6*A*), where DMI has nil impact on the seasonal components of rainfall (Figure 6*B*) but is positively associated with the interannual components of rainfall (Figure 6*C*).

DISCUSSION

Moran effects have seldom been observed in population dynamics [2, 3]. This could reflect the dominance of endogenous feedbacks over exogenous forcing in population dynamics [19]. For example, in diseases, a decaying synchrony with distance, or travelling waves of transmission, has been described for both vectorborne diseases [20] and directly transmitted diseases [21]. In contrast, we found that both seasonal and interannual cycles of malaria have a nondecaying synchrony, both in 2-dimensional distance and along an altitudinal gradient, at distances far greater than the mosquito vector dispersal, which on average barely exceeds 2 km [22], or children movement in the area [23]. Moreover, the degree of synchrony in malaria time series is slightly above, yet not statistically different, from rainfall synchrony, as expected under a Moran effect [3].

A Moran effect in malaria transmission at the LVB could be explained by the monotonic dependence of *Plasmodium* parasite transmission on *Anopheles* vector density in endemic areas [4]. Mosquito population regulation is sensitive to the availability and stability of larval habitats [5, 24]. In fact, *Anopheles* vector density tracks rainfall variability in LVB in a regular fashion [12]. It takes about 2 months for malaria transmission to reach its peak following large rainfall events, roughly the total time of a few mosquito generations [25], including the parasite incubation period [26]. This probably implies a reactive response by mosquitoes to the transient creation of habitats by rainfall, assuming a density-dependent

regulation [14], a pattern described in other species of mosquitoes vector of pathogens. Because *Anopheles* mosquitoes are ubiquitous in LVB [5, 12, 24], a synchronized amplification of their populations and malaria transmission following rainfall could explain the patterns of synchrony we report here. If this is the case, then the IOD, which has the strongest impact on rainfall at high altitudes according to climatic circulation models [8], could drive the Moran effect in malaria transmission in LVB, probably by homogenizing rainfall synchrony across the altitudinal gradient, thus homogenizing weather conditions that increase mosquito productivity [24]. The existence of Moran effects in malaria transmission is a pattern that shows the nontrivial impacts of climatic variability on malaria epidemics. For example, the spatial extent of synchronous patterns in malaria transmission (ie, the maximum distance over which malaria synchrony is constant) could be used as indicator of the minimum spatial scale for interventions aimed at eliminating malaria from a given landscape. Thus, consideration of impacts by environmental variability on malaria transmission biology is required to increase robustness in the development and implementation of malaria control and elimination programs, to be prepared against surprises that can arise from malaria forcing by climatic variability, one of the many aspects shaping the complexity of malaria transmission.

Supplementary Data

Supplementary materials are available at *The Journal of Infectious Diseases* online (http://www.oxfordjournals.org/our_journals/jid/). Supplementary materials consist of data provided by the author that are published to benefit the reader. The posted materials are not copyedited. The contents of all supplementary data are the sole responsibility of the authors. Questions or messages regarding errors should be addressed to the author.

Notes

Acknowledgments. We thank R. Snow for providing hospital and meteorological data for Kericho. We also thank the staff at the Kendu Bay, Maseno, Kisii, and Kapsabet hospitals for their help with data compilation.

Financial support. This work was funded by the Japan Society for the Promotion of Science and a Nagasaki University Cooperative Research Grant to L. F. C., M. H., and N. M. Research and page charges were covered by Nagasaki University GCOE program on Tropical and Emergent Infectious diseases. L. F. C. is a Gaikokujin Fellow of Japan Society for the Promotion of Science.

Potential conflicts of interest. All authors: No reported conflicts.

All authors have submitted the ICMJE Form for Disclosure of Potential Conflicts of Interest. Conflicts that the editors consider relevant to the content of the manuscript have been disclosed.

References

1. Liebhold A, Koenig WD, Bjørnstad ON. Spatial synchrony in population dynamics. Annu Rev Ecol Evol Syst **2004**; 35:467–90.
2. Ranta E, Lundberg P, Kaitala V. Ecology of populations. Cambridge: Cambridge University Press, **2006**.
3. Blasius B, Stone L. Ecology: nonlinearity and the Moran effect. Nature **2000**; 406:846–7.
4. Smith DL, Drakeley CJ, Chiyaka C, Hay SI. A quantitative analysis of transmission efficiency versus intensity for malaria. Nat Commun **2010**; 1:108.
5. Fillinger U, Sonye G, Killeen GF, Knols BGJ, Becker N. The practical importance of permanent and semipermanent habitats for controlling aquatic stages of *Anopheles gambiae sensu lato* mosquitoes: operational observations from a rural town in western Kenya. Trop Med Intl Health **2004**; 9:1274–89.
6. Drakeley CJ, Carneiro I, Reyburn H, et al. Altitude-dependent and -independent variations in *Plasmodium falciparum* prevalence in northeastern Tanzania. J Infect Dis **2005**; 191:1589–98.
7. Bødker R, Msangeni HA, Kisinza W, Lindsay SW. Relationship between the intensity of exposure to malaria parasites and infection in the Usambara Mountains, Tanzania. Am J Trop Med Hyg **2006**; 74:716–23.
8. Anyah R, Semazzi F, Xie L. Simulated physical mechanisms associated with multi-scale climate variability over Lake Victoria basin in East Africa. Mon Weather Rev **2006**; 134:3588–609.
9. Hashizume M, Terao T, Minakawa N. The Indian Ocean Dipole and malaria risk in the highlands of western Kenya. Proc Natl Acad Sci U S A **2009**; 106:1857–62.
10. Behera SK, Luo J-J, Masson S, et al. Paramount impact of the Indian Ocean Dipole on the East African short rains: a CGCM study. J Climate **2005**; 18:4514–30.
11. Saji NH, Goswami BN, Vinayachandran PN, Yamagata T. A dipole mode in the tropical Indian Ocean. Nature **1999**; 401:360–3.
12. Minakawa N, Sonye G, Mogi M, Githeko A, Yan GY. The effects of climatic factors on the distribution and abundance of malaria vectors in Kenya. J Med Entomol **2002**; 39:833–41.
13. Shanks G, Biomndo K, Hay S, Snow R. Changing patterns of clinical malaria since 1965 among a tea estate population located in the Kenyan highlands. Trans R Soc Trop Med Hyg **2000**; 94:253–5.
14. Chaves LF, Koenraadt CJM. Climate change and highland malaria: fresh air for a hot debate. Q Rev Bio **2010**; 85:27–55.
15. Shumway RH, Stoffer DS. Time series analysis and its applications. New York: Springer, **2000**.
16. Ghil M, Allen MR, Dettinger MD, et al. Advanced spectral methods for climatic time series. Rev Geophys **2002**; 40:1003.
17. Huang NE, Shen Z, Long SR, et al. The empirical mode decomposition and the Hilbert spectrum for nonlinear and non-stationary time series analysis. Proc R Soc London Ser A Math Phys Eng Sci **1998**; 454:903–95.
18. Bjørnstad ON, Falck W. Nonparametric spatial covariance functions: Estimation and testing. Environ Ecol Stat **2001**; 8:53–70.
19. Turchin P. Complex population dynamics. Princeton, NJ: Princeton University Press, **2003**.
20. Cummings DAT, Irizarry RA, Huang NE, et al. Travelling waves in the occurrence of dengue haemorrhagic fever in Thailand. Nature **2004**; 427:344–7.
21. Viboud C, Bjørnstad ON, Smith DL, Simonsen L, Miller MA, Grenfell BT. Synchrony, waves, and spatial hierarchies in the spread of influenza. Science **2006**; 312:447–51.
22. Silver JB. Mosquito ecology: field sampling methods. 3rd ed. New York: Springer, **2008**.
23. Prothero RM. Migrants and malaria. London: Longmans, **1965**.
24. Minakawa N, Omukunda E, Zhou G, Githeko A, Yan G. Malaria vector productivity in relation to the highland environment in Kenya. Am J Trop Med Hyg **2006**; 75:448–53.
25. Bayoh MN, Lindsay SW. Effect of temperature on the development of the aquatic stages of *Anopheles gambiae* sensu stricto (Diptera: Culicidae). Bull Entomol Res **2003**; 93:375–81.
26. Lindsay SW, Birley MH. Climate change and malaria transmission. Ann Trop Med Parasitol **1996**; 90:573–88.